

SUPPORTING INFORMATION

Interrogating Detergent Desolvation of Nanopore-Forming Proteins by Fluorescence Polarization Spectroscopy

Aaron J. Wolfe,^{1,2} Yi-Ching Hsueh,¹ Adam R. Blanden,³
Mohammad M. Mohammad,¹ Bach Pham,⁴ Avinash K. Thakur,^{1,2}
Stewart N. Loh,³ Min Chen,⁴ and Liviu Movileanu^{1,2,5}

¹*Department of Physics, Syracuse University, 201 Physics Building, Syracuse, New York 13244-1130, USA*

²*Structural Biology, Biochemistry, and Biophysics Program, Syracuse University, 111 College Place, Syracuse, New York 13244-4100, USA*

³*Department of Biochemistry and Molecular Biology, State University of New York Upstate Medical University, 4249 Weiskotten Hall, 766 Irving Av., Syracuse, New York 13210, USA*

⁴*Department of Chemistry, University of Massachusetts Amherst, 710 North Pleasant Street, Amherst, Massachusetts 01003-9336, USA*

⁵*Department of Biomedical and Chemical Engineering, Syracuse University, 329 Link Hall, Syracuse, New York 13244, USA*

Running title: Detergent Desolvation of Nanopores

Keywords: FhuA; Single-molecule electrophysiology; Nanopore; Protein engineering; Protein-detergent complex interactions

Correspondence/materials requests:

Liviu Movileanu, PhD, Department of Physics, Syracuse University, 201 Physics Building, Syracuse, New York 13244-1130, USA; Phone: 315-443-8078; Fax: 315-443-9103; E-mail: lmovilea@syr.edu

CONTENTS

- (i) Protein expression and purification under denaturing condition;
- (ii) Protein labeling of FhuA derivatives;
- (iii) Expression, purification, and labeling of OmpG D224C proteins;
- (iv) Contributions of anisotropy values to the Langmuir-Hill isothermal binding curves;
- (v) Secondary structure determination of the refolded FhuA $\Delta C/\Delta 5L$ protein in solution using circular dichroism;
- (vi) Single-channel and macroscopic electrical recordings using planar lipid bilayers;
- (vii) Acquiring equilibrium steady-state endpoints of the FP anisotropy at different concentrations of detergents of varying chemistry;
- (viii) Rotational motions of the protein nanopores under detergent solvation and desolvation conditions;
- (ix) Fluorescence anisotropy readout acquired with LPPG-refolded FhuA $\Delta C/\Delta 5L$ at final refolding detergent concentration of 25 mM;
- (x) Detailed time- and concentration-dependent anisotropy traces acquired with anionic and zwitterionic detergents;
- (xi) Steroidal group-containing detergents are weakly binding to FhuA $\Delta C/\Delta 5L$;
- (xii) Dissociation of maltoside-containing detergents from FhuA $\Delta C/\Delta 5L$;
- (xiii) Dependence of time-dependent, steady-state fluorescence anisotropy on proteins of closely similar structure, but varying isoelectric point;
- (xiv) Current-voltage relationship of FhuA $\Delta C/\Delta 5L$ refolded in detergents of varying chemistry;
- (xv) Stability of the open-state current of the refolded FhuA $\Delta C/\Delta 5L$ proteins at higher applied transmembrane potentials.

1. Protein overexpression and purification of FhuA-based nanopores under denaturing condition.

Through *de novo* synthesis (Geneart, Regensburg, Germany),¹ the *fhua* $\Delta c/\Delta 5l$ gene lacked the regions coding for the cork domain and extracellular loops 3, 4, 5, 10, and 11, as compared to the wild-type *fhua*. *fhua* $\Delta c/\Delta 5l_t7$ was created by inverse PCR² using the forward primer 5'-/Phos/TGC GGG TCG TCC GGA GGT ATT GTG GTT ACC GGT GCC GTT T -3' and the reverse primer 5'-/Phos/GCC AGA TGA ACC TCC ATA TTT AAC GCC CAC TTC ATA CTG-3', using pPR-IBA1-*fhua* $\Delta c/\Delta 5l$ -6 \times His⁺ plasmid as a template. The PCR product was self-ligated to create pPR-IBA1-*fhua* $\Delta c/\Delta 5l_t7$ -6 \times His⁺. This replaced β turn T7 (V³³¹ PEDRP³³⁶) with a single cysteine-containing, flexible, GS-rich peptide loop (GGSSGCGSSGGS). Proteins were expressed in *E. coli* BL21 (DE3). Cells, transformed with pPR-IBA1-*fhua* $\Delta c/\Delta 5l_t7$ -6 \times His⁺ plasmid, were grown in LB media at 37°C until OD₆₀₀ ~0.6-0.7, at which time the protein expression was induced with 0.5 mM isopropyl β -D-1-thiogalactopyranoside (IPTG) and allowed to continue until the cell growth plateaued, as measured by OD₆₀₀. Cells were harvested by centrifugation and the pellet was resuspended in 1X PBS, pH 8.0. The cell lysis was conducted using a microfluidizer, model 110L (Microfluidics, Newton, MA). The homogenate was centrifuged for 20 min at 4,000 \times g and 4°C. Inclusion bodies were resuspended and washed 3 times in 1X PBS, 1% Triton X-100, pH 8.0, followed by centrifugation for 30 min at 30,000 \times g and 4°C. Resulting washed inclusion bodies were resuspended in 50 mM HEPES, 1 mM Tris(2-carboxyethyl)phosphine

(TCEP), 6 M guanidinium hydrochloride (Gdm-HCl), pH 8.0, which was followed by centrifugation at 30,000×g and 4°C to remove the insoluble materials. The final protein-containing solutions were filtered using 0.2 μM filters (Thermo Fisher Scientific, Rochester, NY). The solubilized proteins were loaded onto a column packed with 2 ml of Ni⁺-NTA resin (Bio-Rad, Hercules, CA), which was equilibrated in 200 mM NaCl, 50 mM HEPES, 6 M Gdm-HCl, 1 mM TCEP, pH 8.0. The column was washed in two steps with same equilibrating buffer, but containing 5 and 25 mM imidazole, respectively. The proteins were eluted with equilibrating buffer containing 250 mM imidazole in 5 ml fractions. SDS-PAGE was used to monitor the elution profile of pure proteins (**Supporting Information, Fig. S1**). For the sake of simplicity of mutant abbreviations, “T7” is omitted in the case of all FhuA-based nanopores examined in this study.

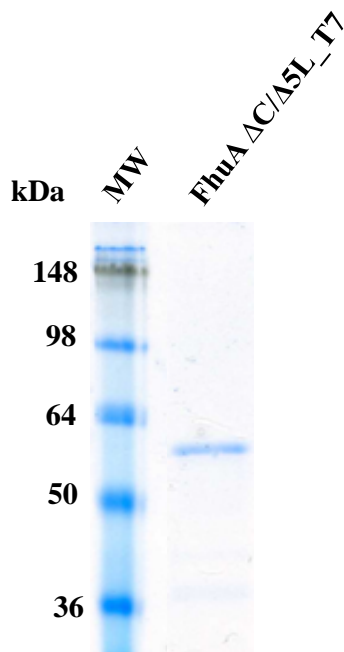


Figure S1: SDS-PAGE gel of purified FhuA ΔC/Δ5L. In this engineered FhuA protein, the β turn 7 (V³³¹PEDRP³³⁶) was replaced by a single cysteine-containing flexible peptide loop (GGSSGCGSSGGS). Proteins were visualized using GelCode Blue Stain Reagent (Thermo Scientific, Rockford, IL). MW stands for molecular-weight standards. For the sake of simplicity of the abbreviations, “T7” was omitted in the case of all FhuA-based protein nanopores examined in this study.

2. Protein labeling of the FhuA derivatives. 10 μM 6×His⁺-tagged FhuA ΔC/Δ5L, FhuA ΔC/Δ5L_25N, and FhuA ΔC/Δ7L_30N proteins were incubated with 200 μM Texas Red C2 maleimide (Thermo Fisher Scientific) overnight at room temperature in 200 mM NaCl, 50 mM Tris, 1 mM TCEP, pH 8.0, and 6 M Gdm-HCl. Proteins were separated from free dye by Ni²⁺-NTA column chromatography in the same buffer, but with a 10-200 mM imidazole step gradient. Labeling stoichiometry was between 0.3-0.8 labels/protein using ε₅₉₅ = 104,000 M⁻¹cm⁻¹ for Texas Red and a correction factor of 0.26 × ε₅₉₅ to account for the dye absorbance at 280 nm.

3. Expression, purification, and labeling of OmpG D224C proteins. OmpG D224C (loop L6) was constructed and expressed in *E. coli*, as previously described.³ Briefly, a single cysteine was introduced to replace the aspartic acid 224 by mutagenesis PCR. BL21 (pLys) *E. coli* cells were transformed with the plasmid pT7-OmpG D224C. Cells were grown in LB medium at 37°C until the OD₆₀₀ reached 0.6 and induced with IPTG (0.5 mM, final concentration). Cells were harvested 3 hours later and lysed in lysis buffer (50 mM Tris·HCl, pH 8.0, 150 mM NaCl, 200 μg/ml lysozyme, 1 mM EDTA, 3 mM TCEP) by sonication. The lysate was centrifuged at 19,000 g for 30 min before washing once with 30 ml 50 mM Tris·HCl, pH 8.0, 1.5 M Urea, 3

mM TCEP. Then the OmpG-containing inclusion body was dissolved in 30 ml 50 mM Tris·HCl, pH 8.0, 8 M Urea, 3 mM TCEP and passed through a 0.45 µm filter before FPLC purification. All OmpG proteins were purified using a 5ml Q-ionic exchange column (GE Healthcare) and eluted in buffer 50 mM Tris·HCl, pH 8.0, 8 M Urea, 3 mM TCEP, 500 mM NaCl by applying a gradient. The purified protein was incubated with 10 mM freshly prepared TCEP for 30 min on ice to reduce the thiols. The TCEP was then removed using a desalting column equilibrated with buffer 50 mM HEPES, pH 7.0, 150 mM NaCl, 8M Urea. Next, the protein was incubated with Texas Red® C₂ Maleimide (Life Technologies Corp) in a molar ratio 1:20 (protein to dye) at room temperature (~23°C) for 2 hours (or at 4 °C overnight). The reaction mixture was passed through the desalting column once again to remove the unreacted chemicals. The sample was snap-frozen in liquid nitrogen and stored at -80°C. To test the foldability of the labeled protein, an aliquot of the sample was then diluted with the refolding buffer 50 mM Tris·HCl, pH 9.0, 3.25% OG until the final concentration of urea reached 3.0 M. Samples were then incubated at 37 °C for 3 days. The refolding efficiency was determined by SDS-PAGE (**Supporting Information, Fig. S2**).

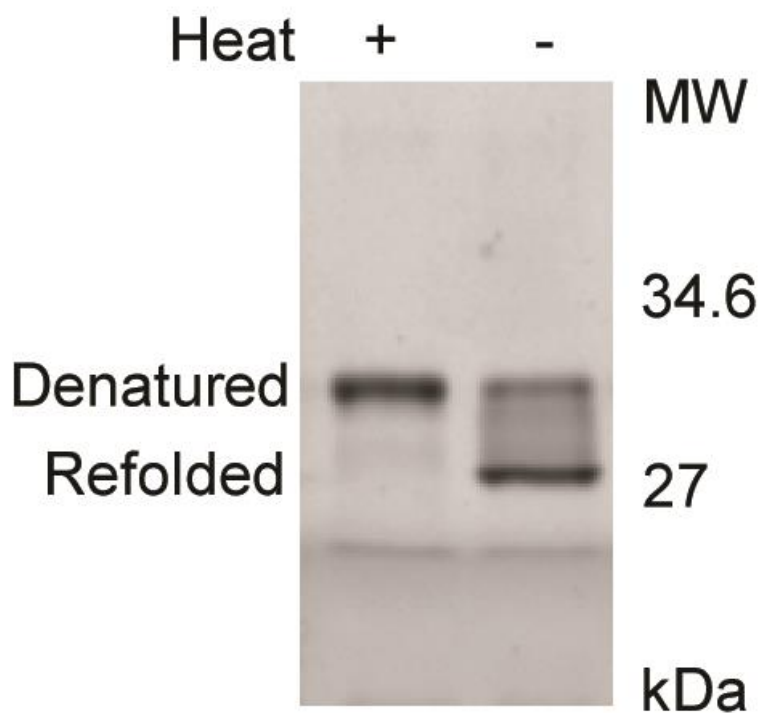


Figure S2: SDS-PAGE analysis of Texas Red labeled OmpG. The refolded OmpG construct was either pre-heated at 95°C for 15 min or directly loaded on a 12.5% SDS-PAGE.³

Table S1: Physical features of the detergents used in this study.

Detergent	FW (Da) ^a	Head group	Aggregation number	CMC (mM) ^b	Micellar weight (kDa)	References
1-lauroyl-2-hydroxy- <i>sn</i> -glycero-3-phosphocholine (LysoFos)	440	Zwitterionic	NA ^c	~0.7 ^d	NA	4
n-dodecyl-N,N-dimethylglycine (LD)	271	Zwitterionic	NA	~1.5 ^e	NA	5
sodium dodecanoyl sarcosine (Sarkosyl)	293	Anionic	2	~14.4 ^f	0.6	6
1-palmitoyl-2-hydroxy- <i>sn</i> -glycero-3-[phospho- <i>rac</i> -(1-glycerol)] (LPPG)	507	Anionic	125	~0.018 ^g	63	4,7
3-[(3-cholamidopropyl)-dimethylammonio]-1-propane sulfonate] (CHAPS)	615	Zwitterionic	~10	~5.9 ^h	6	6
N,N'-bis-(3-D-gluconamidopropyl)cholamide (Big CHAP)	878	Non-ionic	~10	~2.9 ^b	9	6
n-octyl- β -D-glucoside (OG)	292	Non-ionic	~27-100	~25 ^b	25	6
n-octyl- β -D-thioglucoside (OTG)	308	Non-ionic	~189	~9 ^b	58	6
n-dodecyl- β -D-maltoside (DDM)	511	Non-ionic	~78-149	~0.17 ^b	70	6
n-undecyl- β -D-maltoside (UM)	497	Non-ionic	~71	~0.59 ^b	35	8
n-decyl- β -D-maltoside (DM)	483	Non-ionic	~69	~1.8 ^b	33	6
4-cyclohexyl-1-Butyl- β -D-maltoside (CYMAL-4)	481	Non-ionic	~25	~7.6 ^b	12	9

^aFormula weights of the detergent monomers (FW) were reported by Anatrace (<https://www.anatrace.com/>).

^bCMC values or aggregation numbers in water were reported by Anatrace (<https://www.anatrace.com/>).

^cNA stands for not available.

^dCMC value of LysoFos in 140 mM NaCl, 20 mM Tris-HCl, pH 7.2.⁴

^eDetergent monomers are neutral at pH > 6.¹⁰

^fCMC value in ionic solutions is not available.

^gCMC value of LPPG in 100 mM Tris.HCl, pH 8.0.⁴

^hCMC value of CHAPS in 200 mM NaCl.

4. Contributions of anisotropy values to the Langmuir-Hill isothermal binding curves. Our primary assumption is that during the desolvation process the proteins can be found in either bound or unbound state. A single fluorescent protein nanopore produces two distinct values of anisotropy, either bound, r_b , or unbound, r_u . Because anisotropy is an additive property, the overall anisotropy readout is a variable value given by the fraction-weighted sum of the two possible anisotropy values.

If the concentrations of the detergent desolvated and solvated proteins are $[P]$ and $[PD_n]$, respectively, then the total protein concentration, P_{tot} , is given by

$$P_{tot} = [P] + [PD_n] \quad (S1)$$

Therefore, the equilibrium isothermal binding curves undergo changes in $r(c)$, where c is the detergent concentration, as follows,

$$r(c) = \frac{[P]}{P_{tot}} r_u + \frac{[PD_n]}{P_{tot}} r_b \quad (\text{S2})$$

Using equation (S1), we rearrange (S2), as follows:

$$r(c) = \frac{P_{tot} - [PD_n]}{P_{tot}} r_u + \frac{[PD_n]}{P_{tot}} r_b \quad (\text{S3a})$$

$$r(c) = \left(1 - \frac{[PD_n]}{P_{tot}}\right) r_u + \frac{[PD_n]}{P_{tot}} r_b \quad (\text{S3b})$$

Under extremely low detergent concentration conditions, we assume that most of the proteins will be desolvated (e.g., unbound).

Thereby,

$$P_{tot} = [P]; [PD_n] = 0 \quad (\text{S4})$$

$$r(c) = r_u = r_{min} \quad (\text{S5})$$

Equation (S5) indicates that the unbound value of anisotropy is exactly the minimum value of anisotropy, r_{min} .

At detergent concentration much greater than the CMC, we assume that all available proteins are solvated. Therefore,

$$P_{tot} = [PD_n]; [P] = 0 \quad (\text{S6})$$

$$r(c) = r_b = r_{max} \quad (\text{S7})$$

5. Secondary structure determination of the refolded FhuA $\Delta C/\Delta 5L$ protein in solution using circular dichroism. Circular dichroism (CD) spectra were collected using a Spectropolarimeter (Model 420; Aviv Biomedical, Lakewood, NJ) in a 1 cm x 1 cm quartz cuvette. The cuvette contained protein samples at a concentration of $\sim 1 \mu\text{M}$. For temperature melts, samples were heated at $2^\circ\text{C}/\text{min}$, with a 30 s equilibration prior to each 20 s data read at every 1°C with constant magnetic stirring.

6. Single-channel and macroscopic electrical recordings using planar lipid bilayers. Electrical recordings were conducted using planar bilayer lipid membranes (BLMs) were published previously.¹¹ For macroscopic current recordings, FhuA $\Delta C/\Delta 5L$ was added to the *cis* chamber to a final concentration of $\sim 100 \text{ ng}/\mu\text{l}$. $40 \mu\text{l}$ pure and denatured $6\times\text{His}^+$ -tagged FhuA $\Delta C/\Delta 5L$ was 50-fold diluted into 29 mM DDM, 85 mM OG, or 16 mM LysoFos, containing 200 mM NaCl, 50 mM Tris-HCl, 1 mM EDTA, pH 8.0. The diluted protein samples were left overnight at 23° . Aggregated or misfolded proteins were removed by centrifugation for 15 minutes at $16,000\times g$. Current recordings were obtained by using a patch-clamp amplifier (Axopatch 200B, Axon Instruments, Foster City, CA), which was connected to Ag/AgCl electrodes. The *cis* chamber was grounded, so that a positive current represents positive charge moving from the *trans* to *cis* side.

7. Acquiring equilibrium steady-state endpoints of the FP anisotropy at different concentrations of detergents of varying chemistry.

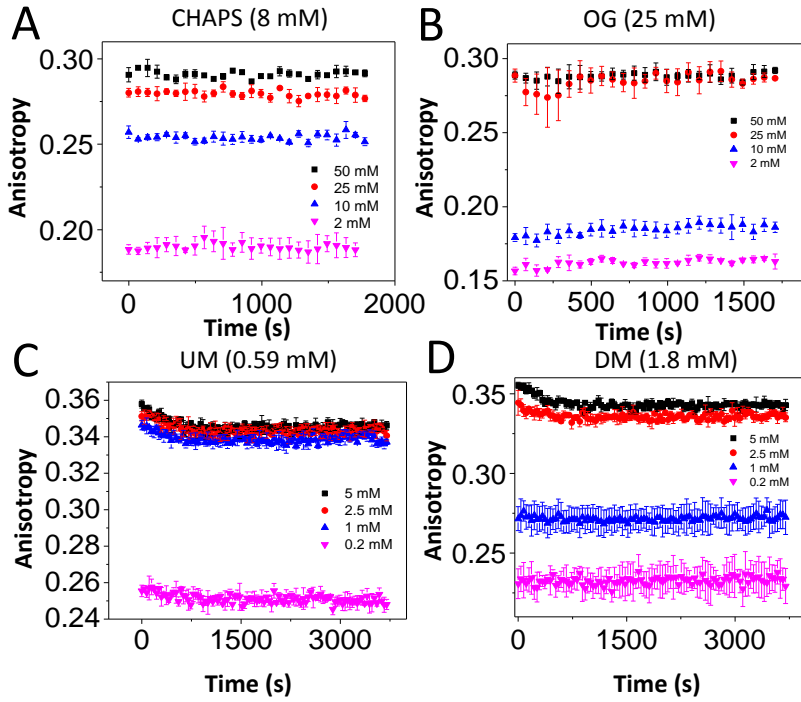


Figure S3: Some examples of concentration-dependent anisotropy endpoints of FhuA $\Delta C/\Delta 5L$ determined after 24 hours incubation at 4°C. (A) CHAPS; (B) OG; (C) UM; (D) DM. The other experimental conditions were the same as in Fig. 2.

8. Rotational motions of the protein nanopores under detergent solvation and desolvation conditions. The steady-state anisotropy measurements can be used to determine the changes in the hydrodynamic radius of the proteins under detergent solvation and desolvation conditions. Specifically, the Perrin equation relates the acquired steady-state fluorescence anisotropy, r , to the rotational diffusion coefficient of the labeled protein, D_r , as follows:^{12,13}

$$\frac{r_0}{r} = 1 + 6D_r\tau_F \quad (\text{S8})$$

where r_0 is the fundamental anisotropy or the theoretical intrinsic maximum anisotropy value. τ_F , the fluorescence lifetime of Texas Red, has a value of 4.2 ns,¹⁴ whereas r_0 is 0.4.¹⁵ On the other hand, the Perrin equation enables the determination of the rotational correlation time, θ , as well as the apparent hydrodynamic volume of the labeled molecule, V_h , according to the following expressions:

$$\theta = \frac{1}{6D_r} \quad (\text{S9})$$

$$V_h = \frac{\theta k_B T}{\eta} = \frac{k_B T}{6\eta D_r} \quad (\text{S10})$$

Here, η denotes the dynamic viscosity of the solution, whereas k_B and T indicate the Boltzmann constant and absolute temperature, respectively. Therefore, we were able to determine the rotational diffusion coefficients of the fully solvated proteins, D_r^{slow} , and detergent desolvation-induced unfolded proteins, D_r^{fast} . Substantial changes in the rotational diffusion coefficients were conceivably determined by alterations in the apparent hydrodynamic radii varying solvation condition. At room temperature, $k_B T = 4.11 \times 10^{-21}$ J. In order to determine the hydrodynamic radii (eq. (5)), we employed a dynamic viscosity, $\eta = 1.028$ mPa s.¹⁶ The average maximum hydrodynamic radii, R_h^{max} , which corresponded to the fully detergent solvated conditions as well as changes in the average hydrodynamic radii between the solvation and desolvation conditions, ΔR_h , were listed in Table S2.

Table S2. Table showing the acquired minima and maxima of anisotropy and rotational diffusion coefficients.^a

Detergent ^b	r_{\min}^c	r_{\max}^c	$D_r^{\text{slow}} (10^7 \text{ s}^{-1})^d$	$D_r^{\text{fast}} (10^7 \text{ s}^{-1})^d$	$R_h^{\text{max}} (\text{nm})^e$	$\Delta R_h (\text{nm})^f$
LysoFos	0.224 ± 0.012	0.329 ± 0.002	0.86 ± 0.03	3.1 ± 0.4	2.7	0.93 ± 0.09
LD	0.228 ± 0.003	0.335 ± 0.001	0.77 ± 0.01	3.0 ± 0.1	2.7	1.0 ± 0.1
Sarkosyl	0.147 ± 0.139	0.337 ± 0.002	0.74 ± 0.03	6.8 ± 0.5	2.8	1.5 ± 0.3
LPPG	0.229 ± 0.037	0.342 ± 0.004	0.67 ± 0.05	3.0 ± 0.9	2.9	1.1 ± 0.2
CHAPS	0.172 ± 0.048	0.292 ± 0.005	1.5 ± 0.1	5.3 ± 2.0	2.2	0.77 ± 0.20
Big CHAP	0.227 ± 0.002	0.315 ± 0.012	1.1 ± 0.2	3.0 ± 0.1	2.5	0.72 ± 0.14
OG	0.162 ± 0.002	0.291 ± 0.002	1.5 ± 0.1	5.8 ± 0.1	2.2	0.81 ± 0.03
OTG	0.185 ± 0.010	0.277 ± 0.001	1.8 ± 0.1	4.6 ± 0.4	2.1	0.57 ± 0.05
DDM	0.196 ± 0.054	0.336 ± 0.003	0.76 ± 0.04	4.1 ± 1.7	2.8	1.2 ± 0.2
UM	0.230 ± 0.015	0.357 ± 0.003	0.48 ± 0.03	2.9 ± 0.4	3.2	1.5 ± 0.2
DM	0.190 ± 0.033	0.373 ± 0.002	0.29 ± 0.02	4.4 ± 1.2	3.8	2.3 ± 0.2
CYMAL-4	0.231 ± 0.019	0.395 ± 0.001	0.05 ± 0.01	2.9 ± 0.5	6.8	5.1 ± 0.5
SDS ^g	~ 0.16	~ 0.16	~ 0.057	~ 0.057	NA ⁱ	NA ⁱ
Gdm-HCl ^h	~ 0.16	~ 0.16	~ 0.057	~ 0.057	NA ⁱ	NA ⁱ

^aTo reach low detergent concentrations below CMC, the Gdm-HCl-solubilized FhuA $\Delta C/\Delta 5L$ protein was refolded at various detergent concentrations above CMC. These values were stated in **Experimental Methods**.

^bFull names of the detergents are provided in **Experimental Methods**.

^cExperimentally determined anisotropy minima (r_{\min}) and maxima (r_{\max}) for various detergents. r_{\min} was extrapolated for the lowest detergent concentration in the well. r_{\max} was determined for detergent concentrations above the CMC.

^d D_r^{slow} and D_r^{fast} indicate the rotational diffusion coefficients of the FhuA $\Delta C/\Delta 5L$ protein under solvation and desolvation conditions, respectively. Rotational diffusion coefficients were calculated using Perrin's equation (3)¹²⁻¹⁴ for steady-state FP spectroscopy using the theoretical limiting anisotropy, $r_0 = 0.4$,¹⁵ and the fluorescence lifetime for the Texas Red fluorophore, $\tau_F = 4.2 \text{ ns}$.¹⁴

^e R_h^{max} are the maximum hydrodynamic radii of the FhuA $\Delta C/\Delta 5L$ proteomicelle with various solubilizing detergents.

^f ΔR_h is the decrease in the hydrodynamic radius, R_h , as a result of the detergent desolvation-induced unfolding transition of the protein.

^gThe lowest anisotropy, r_1 , which was determined at a denaturing detergent concentration of 40 mM sodium dodecyl sulfate (SDS) (**Fig. 2E**). CMC of SDS is in the range $1.2-7.1 \times 10^{-3} \text{ M}$ depending on the ionic concentration of the buffer solution.⁹

^hThe lowest anisotropy, r_1 , which was determined in 6 M Gdm-HCl.

ⁱNA stands for not applicable.

Table S3. Table showing the fitting parameters derived from dose-response dissociation phases of detergent tori from FhuA $\Delta C/\Delta 5L$. The FP measurements were conducted using a buffer that contained 200 mM NaCl, 50 mM HEPES, pH 7.4 and at a temperature of 24°C. All data are derived as averages \pm SDs of three independent data acquisitions.

Detergent	p	Adj. R-squared ^a	q^b (mM ⁻¹)	K_d^c (mM)
LysoFos	~9.6	0.980	0.538	0.47 \pm 0.07
LD	~81	0.994	1.241	1.8 \pm 0.9
Sarkosyl	1.5 \pm 0.4	0.971	0.139	~0.51
LPPG	~4.5	ND ⁱ	13.8	0.009 \pm 0.003
CHAPS	1.7 \pm 0.6	0.966	0.015	3.4 \pm 1.8
Big CHAP	1.4 \pm 0.6	0.997	0.001	25 \pm 4
OG	5.3 \pm 0.9	0.995	0.013	13 \pm 1
OTG	2.5 \pm 1.1	0.927	0.009	6.2 \pm 2.4
DDM	1.1 \pm 0.3	0.974	0.073	0.52 \pm 0.36
UM	3.5 \pm 0.9	0.935	0.381	0.29 \pm 0.05
DM	1.6 \pm 0.3	0.982	0.007	1.3 \pm 0.4
CYMAL-4	4.4 \pm 1.1	0.997	0.026	6.8 \pm 0.9

^aThis column indicates the adjusted R-squared, which is a modified R-squared that has been adjusted by the number of predictors in the fitting model.

^bThe slope factor or transition steepness was calculated at the midpoint of the dissociation phase. See equations (3)-(5).

^cThe apparent dissociation constant, K_d , was determined as the midpoint of the dose-dependent dissociation phase (e.g., c_0).¹⁷

9. Fluorescence anisotropy readout acquired with LPPG-refolded FhuA $\Delta C/\Delta 5L$ at a final refolding detergent concentration of 25 mM.

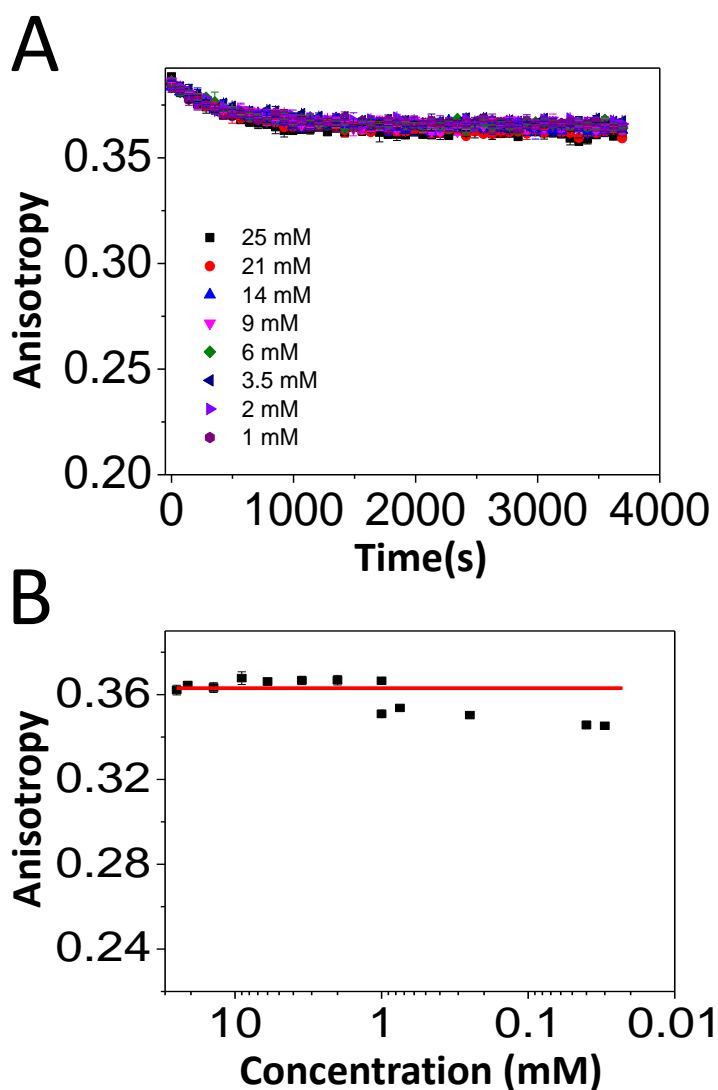


Figure S4: Specific fluorescence anisotropy signature of LPPG-refolded FhuA $\Delta C/\Delta 5L$ at higher detergent concentrations. (A) Time-dependent fluorescence anisotropy of LPPG-refolded FhuA $\Delta C/\Delta 5L$ at a detergent concentration of 25 mM; (B) Dose-response of the endpoints of the PDC interfacial reaction after 24 hours at LPPG concentrations in the range 20 μ M – 25 mM. All the other experimental conditions were the same as in Fig. 2.

10. Detailed time- and concentration-dependent anisotropy traces acquired with anionic and zwitterionic detergents.

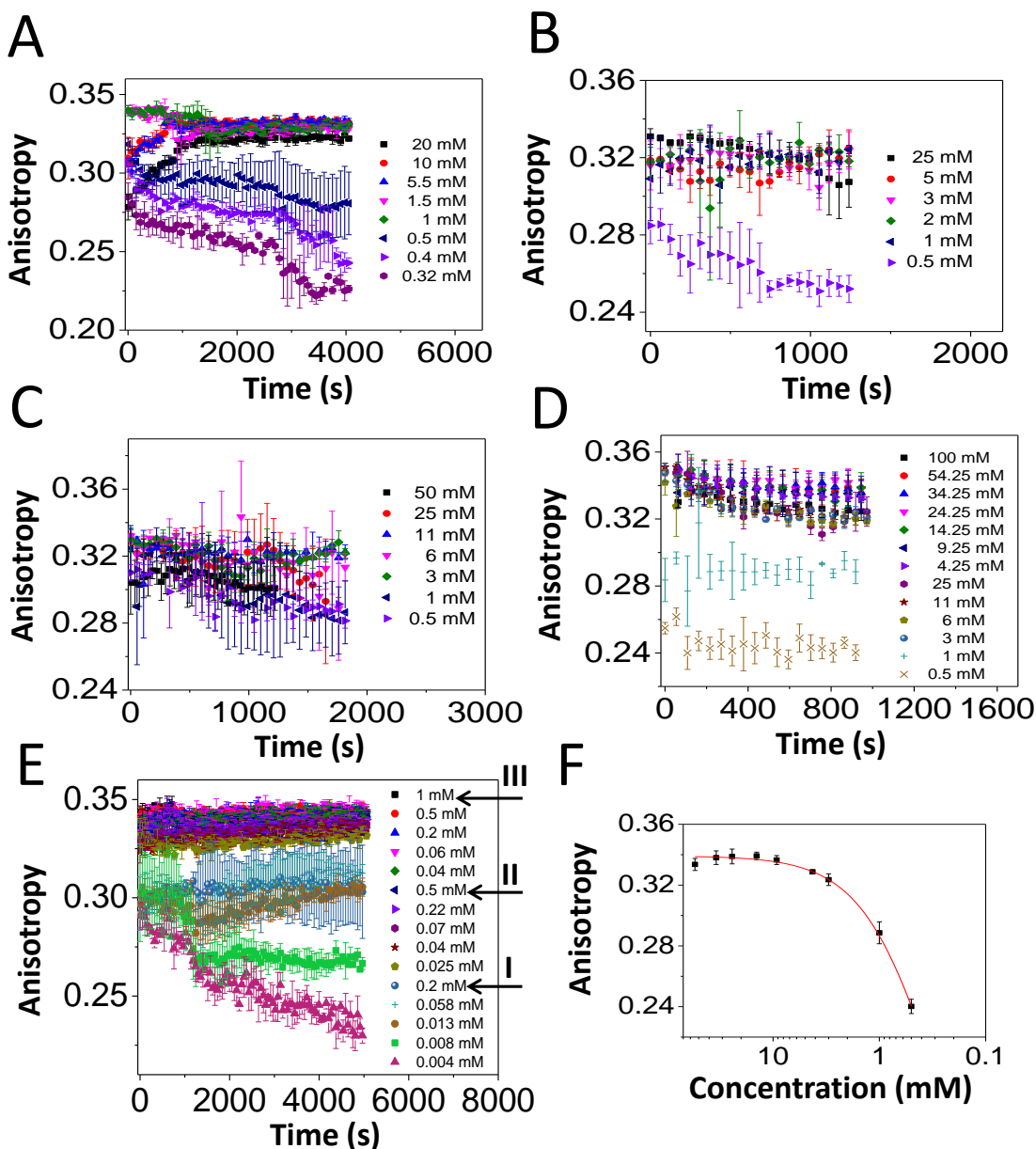


Figure S5: Time- and concentration-dependent anisotropy traces acquired with anionic and zwitterionic detergents. The anisotropy data was acquired by adding overnight refolded protein to a bath of varying detergent concentration. All anisotropy measurements were carried out in 200 mM NaCl, 50 mM HEPES, pH 7.4, and at various detergent concentrations. Detergents started at concentrations above the CMC and were diluted to concentrations below the CMC (**Experimental Methods**). Time-dependent anisotropy measurements were conducted directly after dilution of the refolded protein sample in respective detergent concentration. Final protein concentration was always maintained at 28 nM. The starting detergent concentrations were as follows: **(A)** 20 mM 1-Lauroyl-2-hydroxy-*sn*-glycero-3-phosphocholine (LysoFos); **(B)** 5 and 25 mM n-Dodecyl-N, N-Dimethylglycine (LD); **(C)** 50 mM Sodium dodecanoyl sarcosine (Sarkosyl); **(D)** 50 mM Sarkosyl read after additional 24 hour incubation at 4°C. This is shown, because first read (**C**) did not show clearly defined groups. Here, Sarkosyl refolding starting conditions were 25 mM and 100 mM; **(E)**

0.2, 0.5, and 1 mM 1-palmitoyl-2-hydroxy-*sn*-glycero-3-[phospho-*rac*-(1-glycerol)] (LPPG). The horizontal arrows indicate the three distinct families of curves that correspond to refolding detergent concentrations of 0.2 (I), 0.5 (II), and 1 mM (III); (F) The concentration-response anisotropy data of Sarkosyl, which was fitted by a four-parameter Hill equation. At concentrations near CMC, there are long-lived anisotropy fluctuations, encompassing time-dependent increasing and decreasing phases. We interpret that these phases reflect different populations of detergent-associating (e.g., anisotropy increasing) and detergent-dissociating proteins (e.g., anisotropy decreasing).

11. Steroidal group-containing detergents are weakly binding to the FhuA $\Delta C/\Delta 5L$ nanopore.

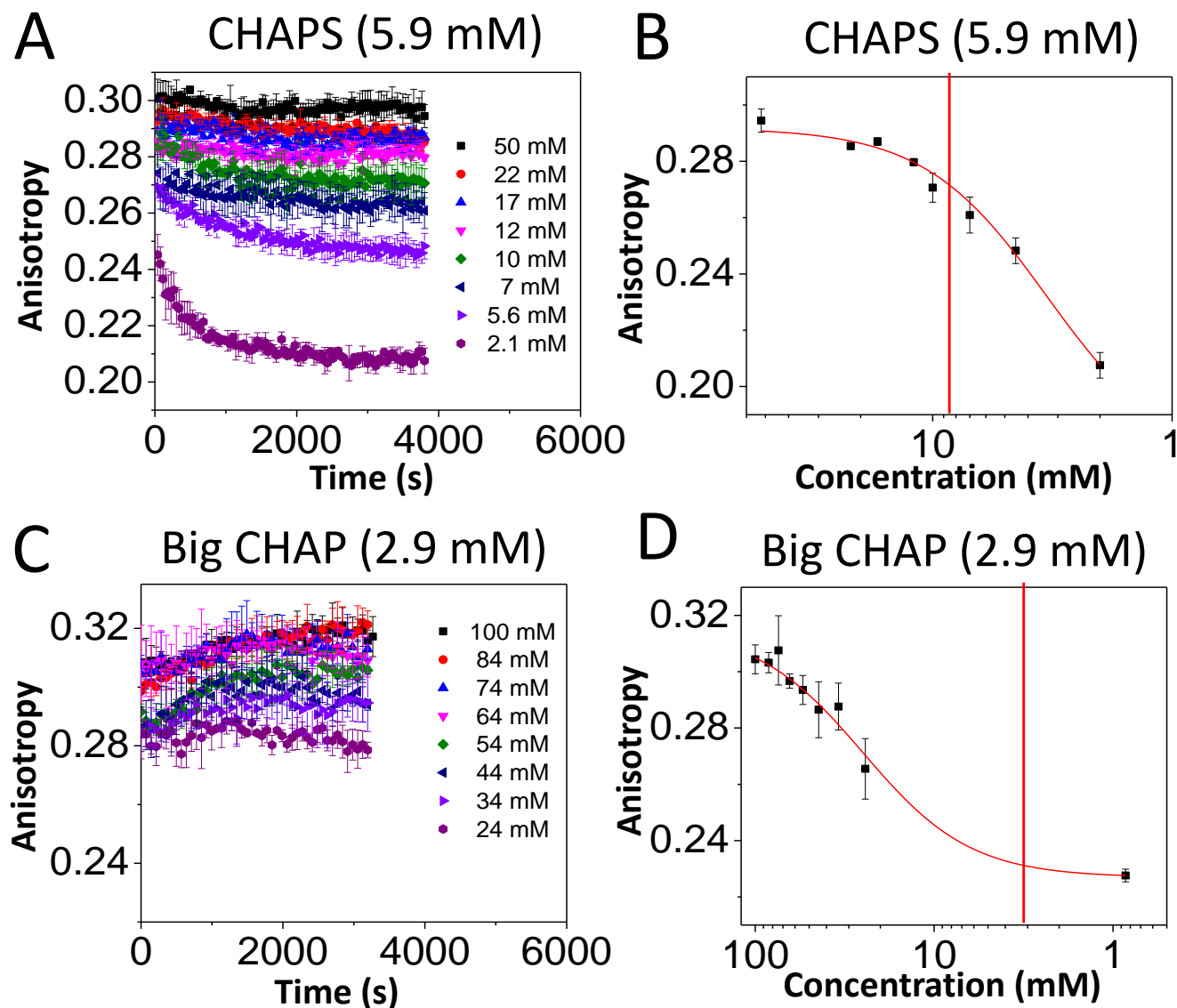


Figure S6: Time-dependent changes in anisotropy produced by the dissociation of steroidal group-containing detergents from FhuA $\Delta C/\Delta 5L$. (A) Time-dependent anisotropy for a starting concentration of 50 mM CHAPS; (B) Concentration-response anisotropy changes observed with CHAPS, whose data points were collected after 24 hours of the dissociation phase; (C) Time-dependent anisotropy for a starting concentration of 100 mM Big CHAP; (D) Concentration-response anisotropy changes observed with Big CHAP. The top of each panel or vertical bars indicate the CMC (Table S1). All the other experimental conditions were the same as in Fig. 2.

12. Dissociation of maltoside-containing detergents from *FhuA* $\Delta C/\Delta 5L$.

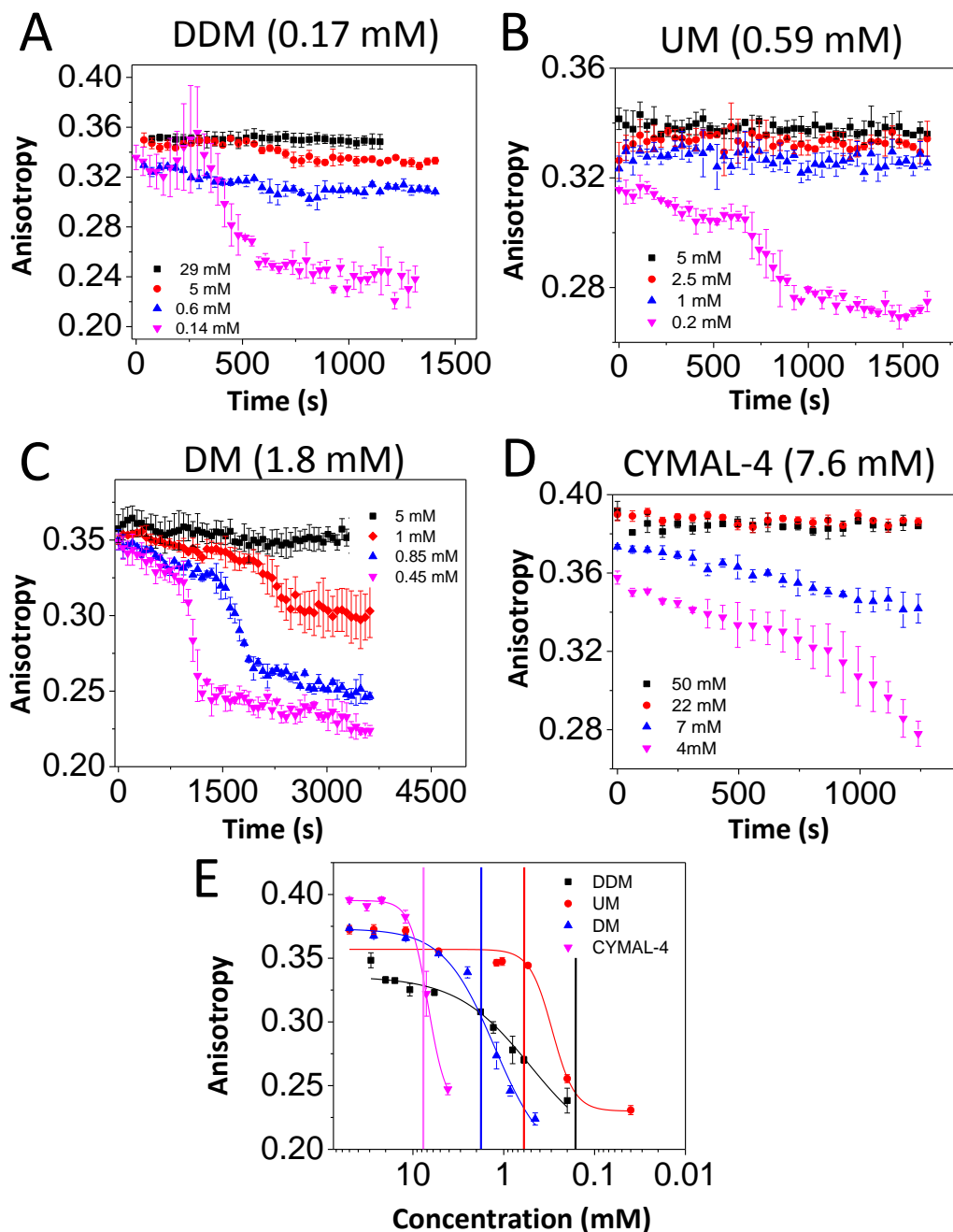


Figure S7: Time-dependent changes in anisotropy produced by the dissociation of neutral, maltoside-containing detergents of varying tail from *FhuA* $\Delta C/\Delta 5L$. The starting detergent concentrations were, as follows: **(A)** 5, 20, and 50 mM DDM, **(B)** 5, 20, and 50 mM UM, **(C)** 5, 20, and 50 mM DM, and **(D)** 50 mM CYMAL-4. **(E)** Concentration-response anisotropy changes observed for maltoside-containing detergents. The top of each panel or vertical bars indicate the CMC (**Table 1**). All the other experimental conditions were the same as in **Fig. 2**. For DM, we were not able to use the four-parameter Hill equation to obtain a statistically significant fit. Instead, we fitted the experimental data points with an asymmetrical five-parameter Hill curve:

$$r(c) = \frac{r_{max} + r_{min} \left\{ \left[1 + \left(\frac{c_0}{c} \right)^p \right]^s - 1 \right\}}{\left[1 + \left(\frac{c_0}{c} \right)^p \right]^s} \quad (\text{S11})$$

where $s=0.071$ is an exponential constant accounting for the asymmetry of the sigmoidal curve. The other parameters in eq. (S11) were the same as those defined above for eqs. (3)-(4) in the text.

13. Dependence of time-dependent, steady-state fluorescence anisotropy on proteins of closely similar structure, but varying isoelectric point.

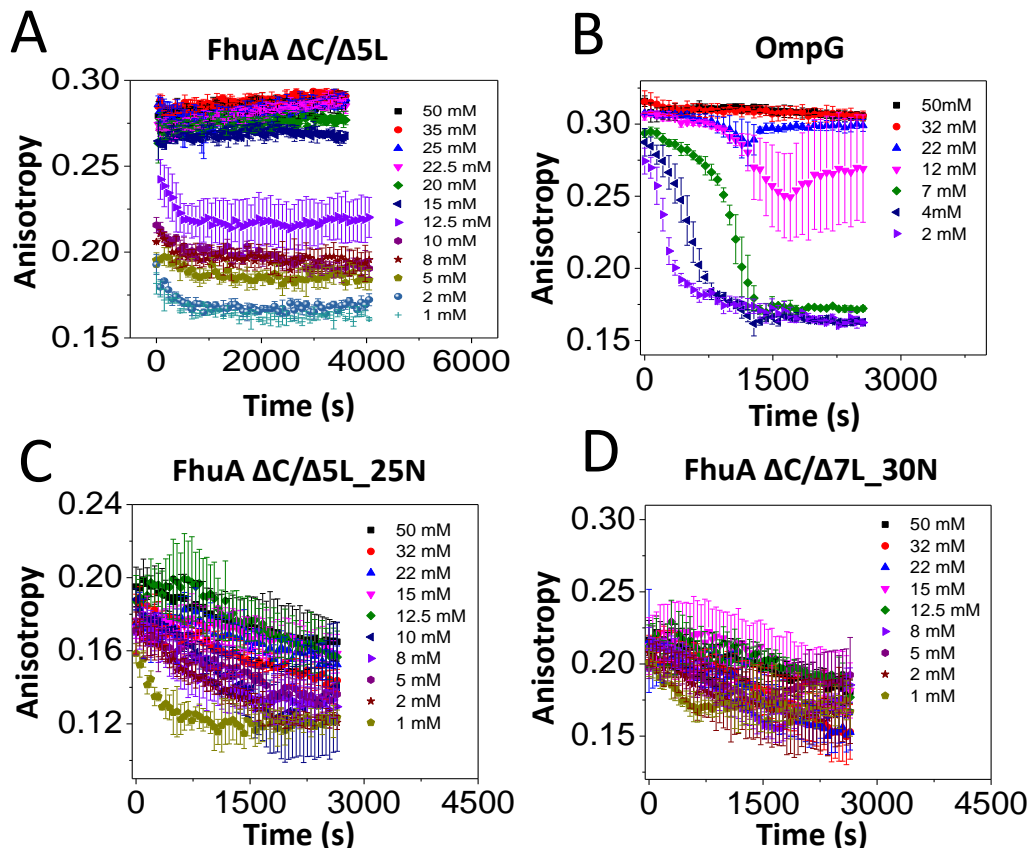


Figure S8: Time- and concentration-dependent anisotropy traces acquired with OG using four protein nanopores: FhuA $\Delta C/\Delta 5L$, OmpG, FhuA $\Delta C/\Delta 5L_{25N}$, and FhuA $\Delta C/\Delta 7L_{30N}$. The other experimental conditions were the same as in Fig. 2.

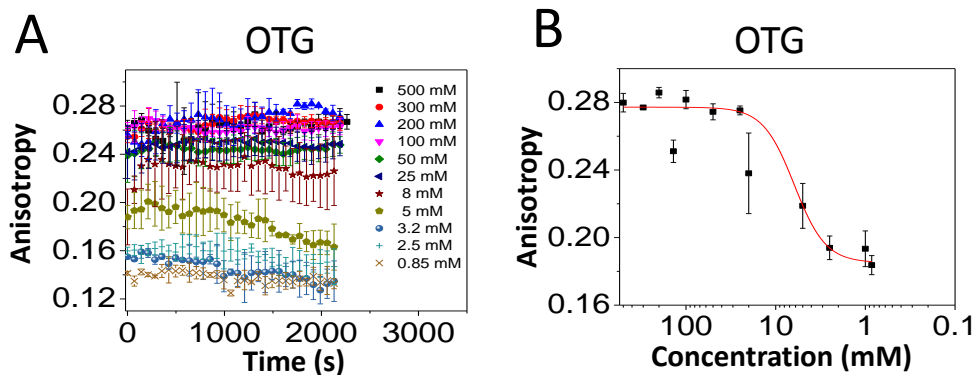


Figure S9: Time- and concentration-dependent anisotropy traces acquired with FhuA $\Delta C/\Delta 5L$ in OTG. The other experimental conditions were the same as in Fig. 2.

14. Current-voltage relationship of FhuA Δ C/ Δ 5L refolded in detergents of varying chemistry. We also noticed unitary conductance values of DDM-refolded FhuA Δ C/ Δ 5L proteins that were lower than 3 nS or greater than 5 nS (~11% and 4%, respectively). These histograms also revealed that 20% OG-refolded FhuA Δ C/ Δ 5L proteins showed a single-channel conductance smaller than 3 nS, whereas only 3% displayed a single-channel conductance greater than 5 nS. Channels under these categories were excluded from further data analysis. The slopes of the current-voltage (I/V) plots recorded with DDM-, OG- and LysoFos-refolded proteins provided values of ~3.9 nS, ~4.4 nS, and ~4.3 nS, respectively (**Fig. S10A**). Similar I/V plots were also obtained from a voltage ramping, between -140 and +140 mV. The slopes gave the unitary conductance values of ~3.9 nS, ~4.4 nS, and ~4.2 nS for DDM-, OG- and LysoFos-refolded proteins, respectively (**Fig. S10B**).

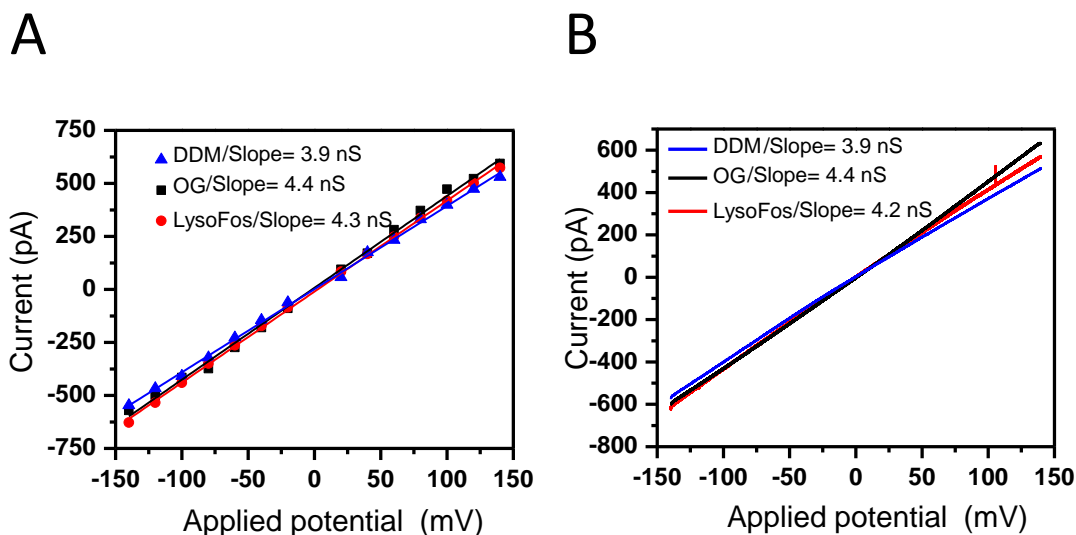


Figure S10: Single-channel electrical signature of the engineered FhuA Δ C/ Δ 5L protein pores refolded in different detergents. (A) The relationship between current and voltage (I/V) of single protein pore insertions from -140 mV to +140 mV for the three proteins. The single-channel conductance values were derived using the I/V slopes. Error bars were omitted for the sake of clarity; (B) Single-channel currents from single channels of the three proteins under a voltage ramp from -140 to +140 mV. The speed of the voltage ramping was 1.4 mV s⁻¹. The single-channel conductance values were derived using the I/V slopes. In A, the single-channel electrical traces were low-pass Bessel filtered at 2 kHz. In B, the single-channel electrical traces were low-pass Bessel filtered at 0.1 kHz to eliminate the current noise generated by the patch-clamp amplifier during the application of the voltage ramp. The single-channel electrical recordings were collected under symmetrical buffer solutions on both sides of the chamber containing 1M KCl, 10 mM potassium phosphate, pH 7.4. For single-channel recordings, 40 μ l pure and denatured 6 \times His⁺-tagged FhuA Δ C/ Δ 5L was 50-fold diluted into 29 mM DDM, 85 mM OG, or 16 mM LysoFos, containing 200 mM NaCl, 50 mM Tris-HCl, 1 mM EDTA, pH 8.0. The dilution ratio of the sample of refolded protein within lipid bilayer chamber was ~1/1000. Therefore, the final detergent concentration in the bilayer chamber did not affect the stability of the membrane.¹⁸

15. Stability of the open-state current of the refolded FhuA Δ C/ Δ 5L proteins at higher applied transmembrane potentials. We examined the refolded FhuA Δ C/ Δ 5L proteins at transmembrane potentials in the ranges -140 to -80 mV and +80 to +140 mV. In 1 M KCl, 10 mM potassium phosphate, pH 7.4, the refolded proteins were stable up to \pm 140 mV (**Fig. S11I-III**). These refolded FhuA Δ C/ Δ 5L proteins showed some reversible short-lived current fluctuations (**Fig. S11**). In the case of the OG-refolded proteins, the single-channel current trace was accompanied by highly infrequent millisecond-time scale, voltage-independent current fluctuations (~0.01 s⁻¹) (**Fig. S11II**). In this work, single-channel electrical recordings performed on the DDM-, OG- or LysoFos-refolded FhuA Δ C/ Δ 5L produced uniform channels with high conductance ~4.0 nS in 1 M KCl (**Fig. 4C and Fig. 4D**). Refolded FhuA Δ C/ Δ 5L proteins showed very stable channel properties at higher

voltages, displaying no major current fluctuations or channel closures (**Fig. S11**). DDM-refolded FhuA $\Delta C/\Delta 5L$ protein was stable up to -120 mV and $+140$ mV (**Fig. S11CI, DI**), OG-refolded FhuA $\Delta C/\Delta 5L$ protein was stable up to ± 140 mV (**Fig. S11DII**), and LysoFos-refolded FhuA $\Delta C/\Delta 5L$ protein was stable up to -100 and $+140$ mV (**Fig. S11BIII, DIII**). The stability and uniformity of channels produced by refolded proteins in different detergents are an advantage. This means that we have options in choosing detergents to refold modified or engineered FhuA proteins in the future. In addition, a uniform conductance may indicate that protein pores, at least for the ones inserted into the bilayer, have one major folded state.^{19,20}

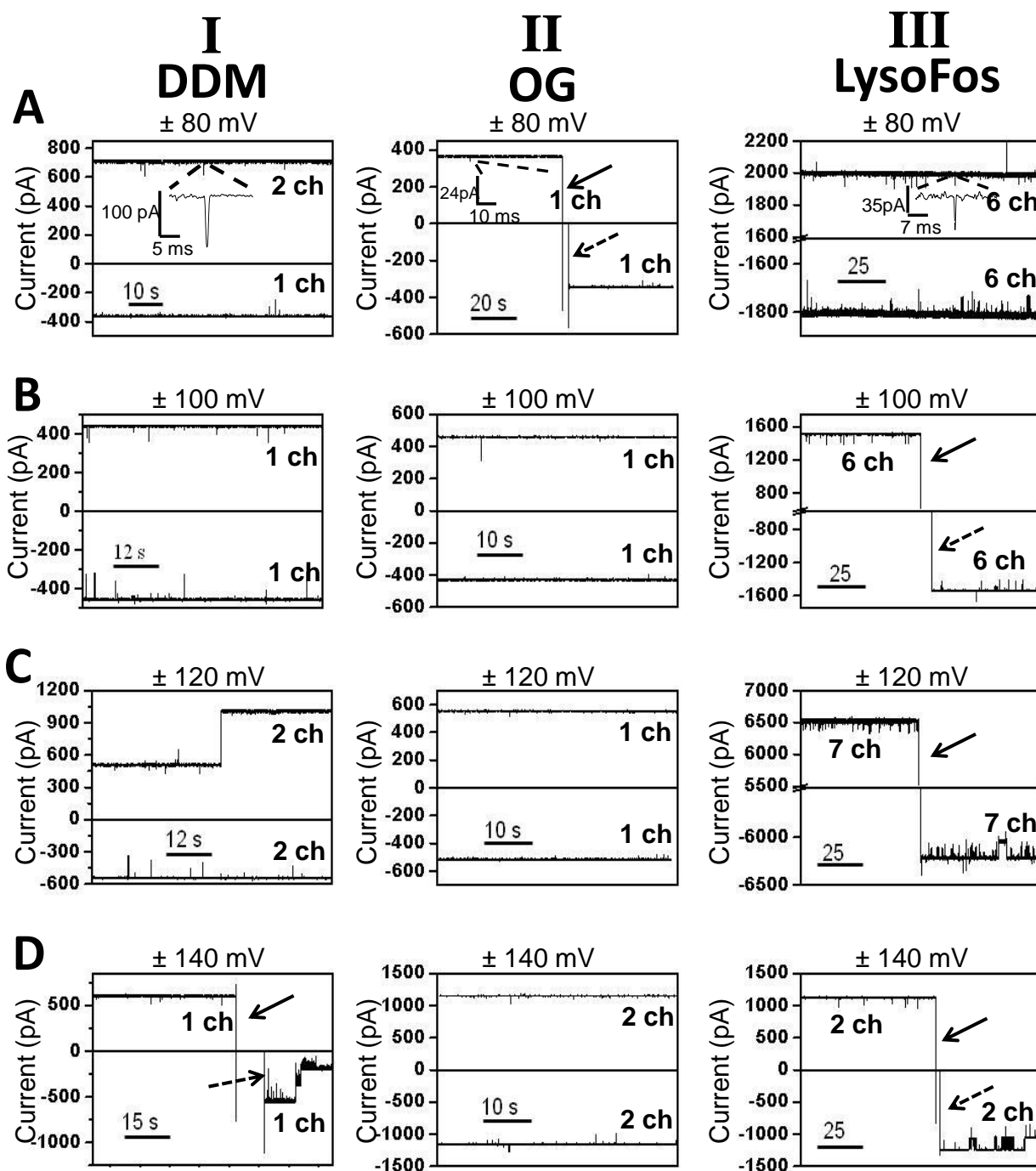
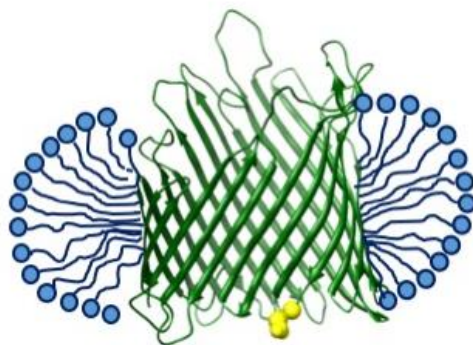


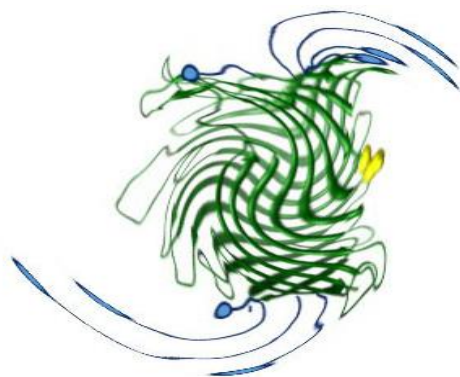
Figure S11: Comparison of the single- and multi-channel electrical traces produced by the FhuA $\Delta C/\Delta 5L$ proteins under various voltages. DDM- (I), OG- (II) and LysoFos-refolded (III) FhuA $\Delta C/\Delta 5L$ protein were reconstituted into planar lipid membranes. The single-channel electrical recordings were collected

under symmetrical buffer solutions on both sides of the chamber containing 1M KCl, 10 mM potassium phosphate, pH 7.4. The number of reconstituted nanopores (e.g., 2 channels is denoted by 2 ch in bold) is indicated near the trace for positive and negative voltages, respectively. Solid and dashed arrows denote the end of the positive voltage and the start of the negative voltage in the same electrical trace, respectively. All electrical traces were low-pass Bessel filtered at 2 kHz. The expanded traces in IA and IIIA indicate representative current spikes recorded at a greater time resolution. The refolding conditions of FhuA $\Delta C/\Delta 5L$ were the same as those mentioned in the caption of **Fig. S10**.

A Detergent-refolded protein
in a prolate proteomicelle



B Desolvation-induced misfolded protein



C Desolvation-induced unfolded protein



Figure S12: Schematic model of the detergent desolvation-induced protein unfolding. This example is for a prolate proteomicelle. **(A)** A nanopore-containing proteomicelle; **(B)** Loss of detergent molecules produces protein misfolding; **(C)** Complete detergent desolvation accelerates protein unfolding as well as reduction in the average hydrodynamic radius, ΔR_h (**Table S2**).

REFERENCES

- (1) Wolfe, A. J.; Mohammad, M. M.; Thakur, A. K.; Movileanu, L. *Biochim. Biophys. Acta* **2016**, *1858*, 19-29.
- (2) Mohammad, M. M.; Howard, K. R.; Movileanu, L. *J.Biol.Chem.* **2011**, *286*, 8000-8013.
- (3) Fahie, M.; Chisholm, C.; Chen, M. *ACS Nano*. **2015**, *9*, 1089-1098.
- (4) Stafford, R. E.; Fanni, T.; Dennis, E. A. *Biochemistry* **1989**, *28*, 5113-5120.
- (5) Parker, J. L.; Newstead, S. *Protein Sci* **2012**, *21*, 1358-1365.
- (6) Linke, D. *Methods Enzymol.* **2009**, *463*, 603-617.
- (7) Lipfert, J.; Columbus, L.; Chu, V. B.; Lesley, S. A.; Doniach, S. *The journal of physical chemistry. B* **2007**, *111*, 12427-12438.
- (8) Oliver, R. C.; Lipfert, J.; Fox, D. A.; Lo, R. H.; Kim, J. J.; Doniach, S.; Columbus, L. *Langmuir* **2014**, *30*, 13353-13361.
- (9) le Maire, M.; Champeil, P.; Moller, J. V. *Biochimica et biophysica acta* **2000**, *1508*, 86-111.
- (10) Neugebauer, J. M. *Methods in enzymology* **1990**, *182*, 239-253.
- (11) Cheneke, B. R.; van den Berg, B.; Movileanu, L. *ACS Chem.Biol.* **2015**, *10*, 784-794.
- (12) Jameson, D. M.; Ross, J. A. *Chemical reviews* **2010**, *110*, 2685-2708.
- (13) Gradinaru, C. C.; Marushchak, D. O.; Samim, M.; Krull, U. J. *Analyst* **2010**, *135*, 452-459.
- (14) Lakowicz, J. R. *Principles of Fluorescence Microscopy*, 2nd ed.; Springer: New York, 2006.
- (15) Prazeres, T. J. V.; Fedorov, A.; Barbosa, S. P.; Martinho, J. M. G.; Berberan-Santos, M. N. *Journal of Physical Chemistry A* **2008**, *112*, 5034-5039.
- (16) Lide, D. R. E. *CRC Handbook of Chemistry and Physics - A Ready Reference Book of Chemical and Physical Data*, The 88th ed.; CRC Press - Taylor and Francis Group: Boca Raton 2008.
- (17) Rossi, A. M.; Taylor, C. W. *Nature protocols* **2011**, *6*, 365-387.
- (18) Mohammad, M. M.; Tomita, N.; Ohta, M.; Movileanu, L. *ACS chemical biology* **2016**, *11*, 2508-2518.
- (19) Arora, A.; Rinehart, D.; Szabo, G.; Tamm, L. K. *J.Biol.Chem.* **2000**, *275*, 1594-1600.
- (20) Tamm, L. K.; Hong, H.; Liang, B. *Biochim.Biophys.Acta* **2004**, *1666*, 250-263.